Anomalous *Z* dependence of a magnetic dipole transition in the Ti I isoelectronic sequence

F. G. Serpa,* E. S. Meyer, C. A. Morgan,† J. D. Gillaspy, J. Sugar, and J. R. Roberts
Atomic Physics Division, National Institute of Standards and Technology, Gaithersburg, Maryland 20899-0001

C. M. Brown and U. Feldman
E. O. Hulburt Center for Space Research, Naval Research Laboratory, Washington, D.C. 20375-5000

In isoelectronic sequences, transition wavelengths ordinarily move rapidly to shorter wavelengths as Z increases. However, it has been predicted that a particular sequence of magnetic dipole ($M1$) transition wavelengths for the Ti-like ions, Xe^{+32} through U^{+70}, remain relatively constant in the 320–400-nm range. In the present paper we extend the experimental identifications of the Ti-like $M1$ transitions from Ba and Xe to Nd (Nd^{+38}) and Gd (Gd^{+42}) to verify this behavior. Using the newly acquired wavelengths to adjust atomic parameters, we have also calculated improved wavelengths for all such $M1$ transitions between Xe ($Z=54$) and Os ($Z=76$).

I. INTRODUCTION

Since it is common for the wavelengths in isoelectronic sequences of ionic transitions to move rapidly to shorter wavelengths as Z increases, wavelengths are typically within the range of optical instruments for only a few members of a sequence. They shift into the vacuum ultraviolet and soft x-ray spectral regions, becoming much more difficult to use as plasma diagnostic probes. Previously, Feldman, Indelicato, and Desclaux [1] reported results from a survey of atomic transitions that violate this general wavelength scaling behavior and that would be suitable for plasma diagnostics in future high-energy Tokamak fusion devices. This search was aimed at finding transitions that fulfill the following requirements: (a) the wavelengths should be ≥250 nm so that transmission optics can be employed; (b) the lines should be reasonably intense and arise from the lowest term of the ground configuration, and (c) the emitting ion should have an ionization potential in the 5–10-keV range. The survey included all promising isoelectronic sequences and was based on calculations using a Dirac-Fock code of Desclaux and co-workers [2,3], including all refinements [4,5]. Feldman, Indelicato, and Desclaux [1] discovered only one set of transitions in only one isoelectronic sequence that fulfilled the stated requirements. They found that the wavelengths of the $M1$, $3d^4\,{}^5D_2-{}^5D_3$ transitions in the Ti-like ions Xe (Xe^{+32}) through U (U^{+70}) are in the 320–400-nm range, satisfying the first requirement. Since the ${}^5D$ is the lowest term of the Ti-like ground configuration, $3d^4$, and since the spontaneous decay rates of the transition are sufficiently high, the second requirement is also fulfilled. The last requirement is fulfilled for all ions with atomic numbers $Z\geqslant75$.

However, *ab initio* calculations often are not sufficiently accurate to unambiguously identify the transition wavelengths when compared with experimental observations, especially where there exists more than one ion stage in the experiment. Therefore, it is necessary to make experimental observations along an isoelectronic sequence in incremental steps to compare with theoretical calculations to assure that further predictions are as accurate as possible.

In a recent paper [6], spectra of highly ionized Xe and Ba in the 320–400-nm range were produced with an electron beam ion trap (EBIT). Each spectrum (see Fig. 1 [6]) contained only two lines, one of which was identified as the predicted Ti-like $M1$ transition, thus providing the first experimental verification of the prediction. The wavelength agreement between the calculations using the Dirac-Fock code of Desclaux and co-workers [2,3] and the experimental values was within 5%, and within 4 nm or 1% with the predictions of the Hartree-Fock code of Cowan [7] when the electrostatic integrals were scaled to 93% of their *ab initio* values. For highly charged ions, the comparison of Cowan's code calculations with experimental values typically requires that the electrostatic integrals be scaled from 90% to 95% of their *ab initio* values [7]. This scaling arises from the interaction of the configuration under investigation with energetically distant perturbers.

In this paper we extend the identification of the Ti-like $M1$ transitions to Nd^{+38} and Gd^{+42}. Using the experimentally acquired wavelengths, we established scaling factors for the electrostatic integrals in the Cowan code for elements $Z=54–76$. From these scaling factors, improved predictions of wavelengths for Ti-like $M1$ transitions within the $3d^4$ ground configuration between Xe ($Z=54$) and Os ($Z=76$) have been obtained.

II. EXPERIMENT

The EBIT at the National Institute of Standards and Technology (NIST), a joint project between NIST and the Naval Research Laboratory (NRL), was used as the source of excited highly charged ions in this work [8,9]. The desired ion stage is produced by successive electron impact ionization from an accelerated electron beam. This beam is produced by

———
*Permanent address: University of Notre Dame, Notre Dame, IN 46556.

†Permanent address: Texas A&M University, College Station, TX 77843.
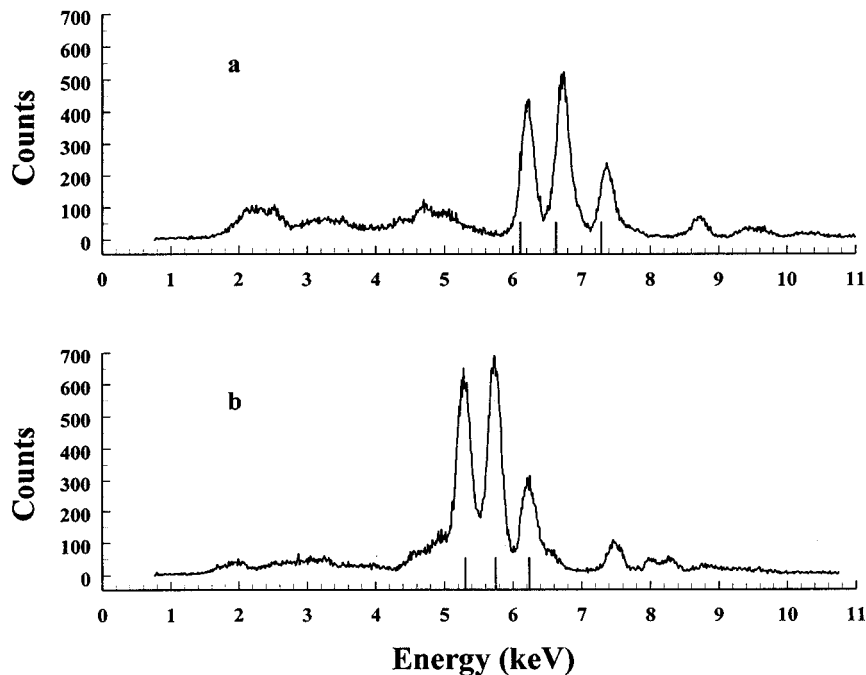
FIG. 1. X-ray spectra in keV of (a) Gd and (b) Nd taken with a Si(Li) detector during injection at 10 kV accelerating potential. The tick marks along the abscissa correspond to calculated transition energies between excited levels and the ground state. The calculations were done with the GRASP[2] code [14].

a electron gun that provides currents up to ~150 mA. A pair of superconducting magnets in a Helmholtz configuration, producing a uniform axial magnetic field of 3 T, compresses the electron beam to a diameter of ~60 μm resulting in a current density of ~5000 A/cm^2. Together the electron beam and the magnetic field produce a radial trap for the ions. Axial trapping of the ions along the electron beam axis is provided by raising the two ends of three collinear, insulated drift tubes to a positive potential with respect to the center drift tube bias potential. Together this results in a cylindrical trap ~30 mm long and ~200 μm in diameter [10] in the direction of the electron beam. A variable voltage between 2 and 20 kV applied to the drift tubes defines an accelerating potential for the electron beam. A correction of approximately -100 eV must be applied to this energy due to the net space charge of the electrons and the positive ions in the trap. The precise energy of the electron beam (~50-eV width) is determined from the variable accelerating potential, the center drift tube bias voltage, and the space-charge correction. By adjusting the accelerating voltage slightly below the ionization energy of the desired ion, the population of a specific charge state can be optimized.

Desired elements are introduced into the trap region in various ways. Due to the composition of the electron gun cathode, Ba is naturally present and is injected slowly in our EBIT. Other elements must be introduced externally either by gas injection or by means of a metal vapor vacuum arc (MEVVA) source. The MEVVA attaches to the top of the EBIT vacuum chamber along the electron beam axis, approximately 1.5 m above the trap region. The operation of the MEVVA has been described in detail previously [11,12]. In brief, the MEVVA consists of a central trigger electrode, a cylindrical cathode, an anode, and extractor plates and is modeled after the Livermore MEVVA design [13]. The composition of the cathode determines the species to be injected. The trigger, cathode, and anode all operate at or slightly above the voltage of the drift tubes to assure that the injected ions will have enough energy to reach the trap. A pulse of

several kilovolts and a few microseconds in duration is applied to the trigger electrode. The resulting discharge generates a small amount of plasma between the cathode and trigger. This plasma, containing low charge states of the species being injected, is accelerated towards the trap. An einzel lens between the MEVVA and the trap provides additional focusing to increase the number of ions arriving at the trap.

A set of eight, 25-mm-high by 2.5-mm-wide, radially positioned slots in the central drift tube provide openings for radiation emanating radially from the trap region. Four 120-mm-diam and four 38-mm-diam knife-edge flanges in the vacuum vessel allow for radial viewing access to the trap region. One of the ports is blocked by a device to suppress the buildup of electrons [8]. A Si(Li) detector, with an energy resolution of ~190 eV, is used to monitor the x-ray spectra through one of the radial ports. This port has a 0.13-mm-thick beryllium window to act as the vacuum interface. Wavelengths above 300 nm were also observed radially through a quartz window port. Wavelength dispersion of this spectra was achieved with a 0.3-m focal length, f/5.3 Czerny-Turner scanning monochromator, with a 1200-groove/mm grating resulting in a reciprocal linear dispersion of 2.6 nm/mm. A low noise, 12-stage, 50-mm-diam, end-on photomultiplier was placed at the monochromator exit slit. A commercial cooler was used to reduce the temperature of the photomultiplier to about $-25\,°$C. This cooling and a magnetic defocuser surrounding the photomultiplier to reduce the active cathode area decreased the detector noise to about 3 counts/s. Because of the detector sensitivity to stray magnetic fields from the EBIT superconducting magnet, two 50-mm-diam (150- and 175-mm focal length) fused silica plano-convex lenses were used to image light from the trap to a new position about 850 mm away from the EBIT. This combination of lenses produced a demagnification of ~0.8 and transmitted ~30% of the light incident on the first lens. The monochromator was attached to an optical table, which was fully adjustable in the horizontal plane, and moved independently from the two lenses. Two translation stages with a
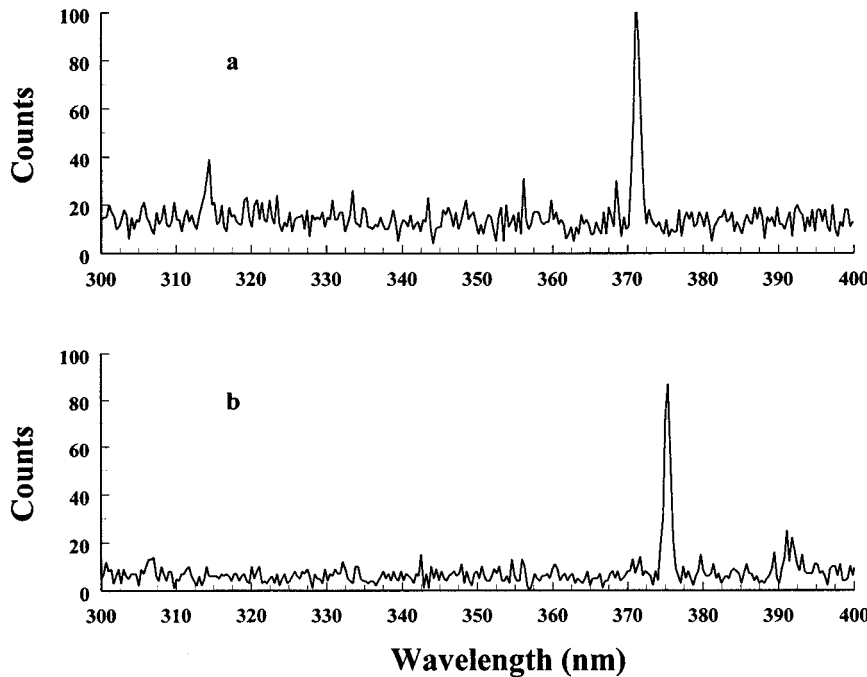
FIG. 2. Survey of emission spectra in the 300–400-nm range obtained with a scanning monochromator for (a) Gd and (b) Nd.

resolution $\leqslant 10$ μm were used to translate the monochromator and optical table assembly and placed the monochromator's entrance slit at the trap image formed by the lenses.

For the present experiment, Gd and Nd where injected separately into the EBIT using the MEVVA. The main accelerating voltage and the MEVVA anode voltage were set to 10 keV, appropriate to produce Ne-like Nd and Gd. The upper, middle, and lower drift tubes were at +500, +100, and +500 V, with respect to the main accelerating voltage. To load the trap with ions, first the upper drift tube offset voltage was reduced to zero, which combined with the offset of +100 V on the middle drift tube, forced any residual ions out of the trap. After 2 ms, a pulse was transmitted through a fiber optic to trigger the MEVVA, and 15 μs later the upper drift tube offset voltage was raised again to +500 V to trap the injected ions. This cycle was repeated about every 2 s and trapping was confirmed by observing the corresponding x-ray spectra.

III. DATA

X-ray spectra of Gd obtained with the Si(Li) detector are shown in Fig. 1(a). The transition energies to the ground state from the $2p^5(^2P_{1/2})3d(1/2,3/2)_1, 2p^5(^2P_{3/2})3s(3/2, 1/2)_1$ and $2p^5(^2P_{3/2})3d(3/2,5/2)_1$ levels (in j-j coupling) of Ne-like Gd were obtained from calculations using the multiconfigurational Dirac-Fock (MCDF) code GRASP[2] [14] and yielded 6.11, 6.63, and 7.29 keV, respectively. This agrees with the main peaks in Fig. 1(a) at 6.2, 6.7, and 7.4 keV. Similar calculations for Ne-like Nd give 5.31, 5.75, and 6.24 keV for the same transitions and are also in agreement with our measured values of 5.34, 5.78, and 6.27 keV [see Fig. 1(b)]. In order to obtain the desired Ti-like charge state, a similar timing sequence of events described above was followed. Ions were injected with a 10-kV accelerating potential, and 3 ms after the upper drift tube bias was raised, the total center drift tube voltage was lowered to the Ti-like

ionization energy. The total duration of each cycle was about 2 s. Wavelength survey scans were made between 300 and 400 nm for Nd and Gd (see Fig. 2). The Gd scan was taken at a 3.34-keV drift tube voltage, a 63-mA electron beam current, and with a 400-μm entrance and exit slit widths. It showed a prominent peak at 371.3 nm [Fig. 2(a)] and a weaker peak at $\sim$314.4 nm [Fig. 2(a)]. The Nd scan was taken at a drift tube voltage of 2.77 keV, 49-mA electron beam current, and 600-μm entrance and exit slits. It showed a main peak at $\sim$375.3 nm and a weaker feature at $\sim$391.0 nm [Fig. 2(b)]. We identified the stronger peaks as the $3d^4\,^5D_2-^5D_3$ $M1$ transition.

By setting the monochromator to the wavelength of the Gd $M1$ peak at 371.3 nm and varying the accelerating potential, we observed the dependance of the line intensity on drift tube potential. A plot of this line intensity is shown in
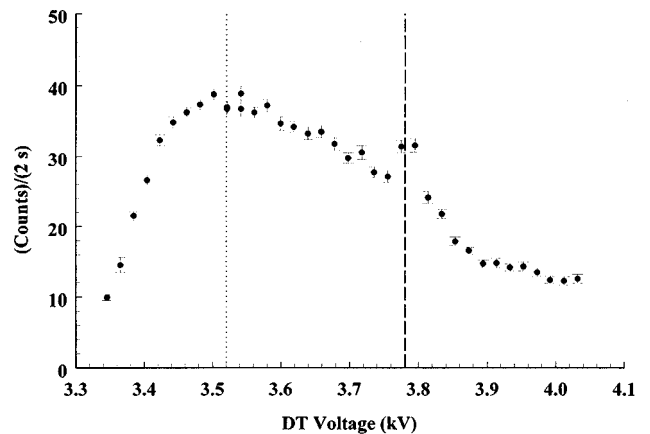
FIG. 3. Detector signal from the $M1$ line of Ti-like Gd as a function of the voltage of the middle drift tube. The dotted line indicates the voltage corresponding to maximum intensity and the dashed line indicates the voltage corresponding to the dielectronic recombination feature.
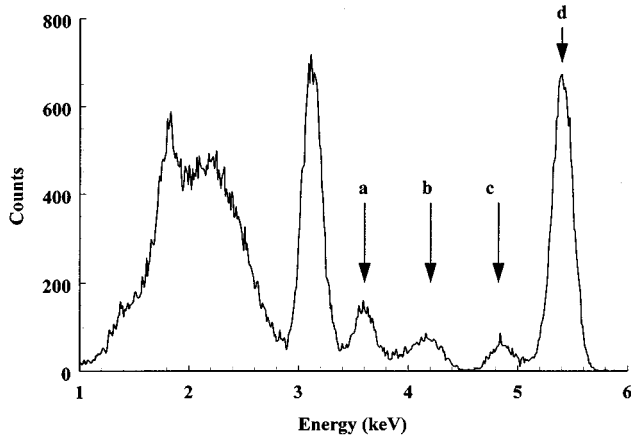
FIG. 4. X-ray spectra in keV of highly ionized Nd observed during the $M1$ line scan. The peaks labeled a and b are consistent with radiative recombination into the $n=5$ and 4 shells, respectively, for Ti-like Nd. The peaks labeled c and d are due to dielectronic recombination into the Ti-like charge state.

TABLE I. Scaling factors and calculated and observed wavelengths for the $3d^4(^5D_2-^5D_3)$ Ti-like $M1$ transitions. All wavelengths are in nm and the uncertainties are listed in parentheses.

Z	Element	Scale factor	$\lambda(2-3)_{calc}$	λ_{expt}
54	Xe	0.922	413.0	413.9(2)[a]
56	Ba	0.930	393.2	393.2(2)[a]
60	Nd	0.946	374.9	375.3(2)[b]
64	Gd	0.962	368.6	371.3(2)[b]
68	Er	0.978	363.6	
72	Hf	0.994	356.2	
74	W	1.000	352.4	
76	Os	1.000	350.7	

[a]Reference [6].
[b]This work.

Fig. 3, where the horizontal axis has been corrected for the 100-V offset applied to the middle drift tube but has not been adjusted for the space-charge effects. The vertical axis shows the detector signal, which has been normalized for temporal variations in the number of trapped ions over the time of acquiring this data. The normalization is derived from the ratio of the peak signals (at 3.52 kV) at the beginning and end of the data acquisition. The data exhibit the expected behavior for the Ti-like charge state, as derived from computer simulations of the charge-state balance in the trap as a function of beam energy [15]. The experimental maximum found at a central drift tube voltage of 3.52 keV is about 100 V higher than the beam energy of the simulation. This is in agreement with an expected space-charge correction of about -100 V. The plot also shows a small peak at higher drift tube voltage. We attribute this to an enhancement of the Ti-like population due to dielectronic recombination (DR) from the Sc-like charge state; the resonant capture of an electron into the $3d$ shell with the excitation of a $2p_{1/2}$ electron to the $3d$ shell would require an electron energy of about 3.69 keV, according to our MCDF calculations. Again this is 100 V lower than the 3.78-keV energy observed and is consistent with our estimate of the space-charge correction.

As a further confirmation of the charge-state identification, an x-ray spectrum taken with the Si(Li) detector during the Nd scan is shown in Fig. 4. The peaks labeled a and b are due to radiative recombination into Ti-like Nd with the captured electron in the $n=5$ and 4 shell, respectively. Our MCDF calculations predict 3.6 and 4.2 keV for peaks a and b, respectively. The peaks labeled c and d are due to DR into the Ti-like charge state, where an electron is captured into the $3d$ shell and a $2p_{3/2}$ electron is excited to the $3d$ shell. The observed energy of peaks c and d agrees with our MCDF calculations for the decay of a $3s$ (4.8 keV) or $3d$ (5.3 keV) electron to fill the hole left in the $2p_{3/2}$ shell by the DR process.

Higher-resolution wavelength scans were made using narrower slit widths to better determine the $M1$ transition wavelengths, as well as to observe other features present at shorter wavelength in Gd. The monochromator wavelength scale

was calibrated by viewing a low-pressure He discharge lamp through the radial viewport located on the side of the EBIT opposite the monochromator. The wavelength range used was 296.7–435.8 nm. Also, by injecting small amounts of Ar and Kr gas into the EBIT, *in situ* calibration lines could be observed. The $Ar^{+23}2s^2 2p^2 P_{1/2}-^2P_{3/2}$ and the $Kr^{+22}3s^2 3p^2\ ^3P_1-^3P_2$ $M1$ transitions were observed at 441.24(2) and 384.09(2) nm, respectively [17]. The wavelength uncertainties determined from these two wavelength calibrations, along with a possible systematic wavelength shift from the data acquisition, were added in quadrature to give an overall uncertainty of $\leq\pm0.2$ nm.

IV. DISCUSSION AND CONCLUSION

For the Gd $3d^4\ ^5D_2-^5D_3$ $M1$ transition, the experimental value differed from its predicted value by about 10 nm when fixed scaling was used for the electrostatic integrals in the Cowan code [7]. To improve the agreement, we used the measured Gd $M1$ line and the previously observed lines (Ref. [6]), and adjusted the electrostatic integrals in the Cowan code by a linear variation of the scale factor$=0.922+0.004(Z-54)$ (see Table I). This gave the best fit to the known wavelengths over the range from $Z=54$ (0.922) to $Z=74$ (1.000). For $Z\geq74$, this factor is set equal to one, i.e., no scaling, due to the far configuration-interaction effects approaching zero at high ionization. This variation of the scale factors not only fit our observed wavelengths but also correctly predicted the wavelength of the $M1$ line for Nd, which we subsequently observed. Such variation of the scale factor for the electrostatic integrals is a commonly observed behavior along an isoelectronic sequence. For example, in the investigation of the Zn sequence by Litzen and Reader [16], similar increases with Z of the scale factor for the electrostatic integrals, F^2, were found. At W, the Cowan code wavelength equals that obtained in Ref. [1] from the Dirac-Fock code of Desclaux and co-workers.

In Gd we also found a weaker peak at 314.4 nm. This peak has a similar beam energy dependence as the $M1$ line, which suggests that it also belongs to this Ti-like charge state. A candidate for this is the $3d^4\ ^5D_4-^5D_3$ $M1$ transition, which competes with the $3d^4\ ^5D_2-^5D_3$ for line strength at high Z [1]. An observation of other members of this isoelectronic sequence is needed to confirm this identification.
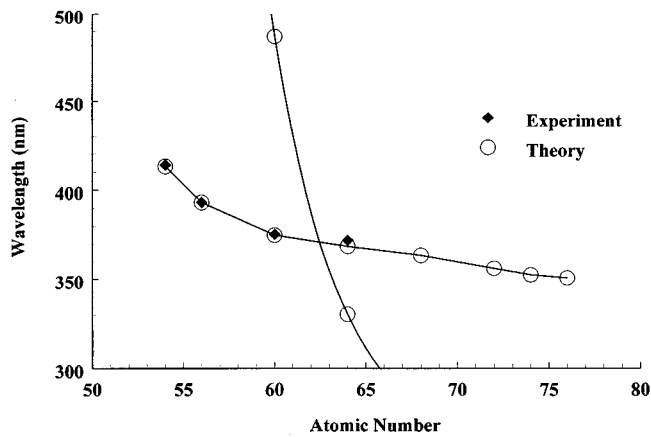
FIG. 5. *Z* dependence of Ti-like $M1$ lines as a function of atomic number. The flatter curve represents the $3d^4\ {}^5D_2$-${}^5D_3$ transitions and the steeper curve represents the $3d^4\ {}^5D_4$-${}^5D_3$ transitions. Open circles correspond to the wavelengths calculated with the scaled Hartree-Fock code of Cowan [7] and the filled diamonds represent experimental observations.

At lower central drift tube potentials, a second weak peak appeared at 320.8 nm, suggesting that it belongs to a lower charge state, e.g., V-like Gd.

Figure 5 is a plot of the calculated wavelengths (open circles) of the $M1$ transitions, $3d^4\ {}^5D_2$-${}^5D_3$ and $3d^4\ {}^5D_4$-${}^5D_3$ obtained with the Hartree-Fock code of Cowan using the scaling in Table I. This figure illustrates the normal behavior of the $M1$ lines as a function of atomic number, i.e., a very rapid change in the wavelengths of the $3d^4\ {}^5D_4$-${}^5D_3$ transitions, while the anomalous Z dependence is portrayed by the small change in the wavelengths of the $3d^4\ {}^5D_2$-${}^5D_3$ transitions. This figure also includes the observed wavelengths (filled diamonds). Table I lists the data for the $3d^4\ {}^5D_2$-${}^5D_3$ transitions, together with the experimental scale factors. Another observation at higher Z (such as W) would help extend and confirm the present isoelectronic sequence of $M1$ lines for the $3d^4$ configuration, and would likely be of great importance for future tokamak diagnostics.

In conclusion, we have measured and identified the $3d^4\ {}^5D_2$-${}^5D_3$ $M1$ transitions for Nd^{+38} and Gd^{+42}. These measurements extend our previous work for $Z=54$ and 56, and confirm the suppressed Z dependance for these $M1$ transition wavelengths along the Ti-like isoelectronic sequence. To date, we know of no *ab initio* calculations that can predict these wavelengths with an accuracy comparable to the scaled Hartree-Fock code of Cowan.

ACKNOWLEDGMENT

[1] U. Feldman, P. Indelicato, and J. Sugar, J. Opt. Soc. Am. B **8**, 3 (1991).

[2] J. P. Desclaux, Comput. Phys. Commun. **9**, 31 (1975).

[3] P. Indelicato, O. Gorceix, and J. P. Desclaux, J. Phys. B **20**, 651 (1987).

[4] O. Gorceix, P. Indelicato, and J. P. Desclaux, J. Phys. B **20**, 639 (1987).

[5] P. Indelicato, J. Phys. (Paris) Colloq. **150**, C-239 (1989).

[6] C. A. Morgan *et al.*, Phys. Rev. Lett. **74**, 1716 (1995).

[7] R. D. Cowan, *The Theory of Atomic Structure and Spectra* (Univ. California Press, Berkeley, California, 1981).

[8] J. D. Gillaspy *et al.*, in *VIth International Conference on Physics of Highly Charged Ions*, edited by P. Richard *et al.*, AIP

Conf. Proc. No. 247 (AIP, New York, 1993), p. 682.

[9] R. E. Marrs, P. Beiersdorfer, and D. Schneider, Phys. Today **47** (10), 27 (1994).

[10] J. D. Gillaspy *et al.*, Phys. Scr., **T59**, 392 (1995).

[11] I. G. Brown *et al.*, Appl. Phys. Lett. **49**, 1019 (1986).

[12] I. G. Brown *et al.*, Rev. Sci. Instrum. **57**, 1069 (1986).

[13] A. M. Levine *et al.*, Phys. Scr. **T22**, 157 (1988).

[14] F. A. Parpia, I. P. Grant, and C. F. Fischer, GRASP^2 (private communication).

[15] D. Knapp (private communication).

[16] U. Litzen and J. Reader, Phys. Rev. A **36**, 5159 (1987).

[17] V. Kaufman and J. Sugar, J. Phys. Chem. Ref. Data **15**, 321 (1986).